

**Preliminary report****Local behaviour of the connector with mechanical coupler and rebar anchor under tension load**Ivan Milićević^{*1)}, Branko Milosavljević¹⁾, Milan Spremić¹⁾, Rastislav Mandić¹⁾, Marko Popović¹⁾¹⁾ University of Belgrade, Faculty of Civil Engineering, Bulevar kralja Aleksandra 73, 11000 Belgrade, Serbia**Article history**

Received: 25 January 2023

Received in revised form:

04 April 2023

Accepted: 24 April 2023

Available online: 22 May 2023

Keywordsmechanical couplers,
reinforcement,
demountable connections,
tension loads,
composite structures**ABSTRACT**

In the past few decades, demountable connectors have often been used for connections in composite and mixed steel-concrete structures to reduce construction time and costs. Furthermore, the application of demountable connectors enables the reuse of structural elements in these structures, which leads to sustainable design and a circular economy. In this paper, the demountable connector is made out of two parts: (1) mechanical coupler and rebar anchor placed in formwork before casting the concrete element, and (2) steel bolt used for connecting steel to the RC element. Although this connector is increasingly being used in contemporary building structures, its behaviour in composite connections is still insufficiently defined. The paper presents the results of experimental tests and numerical analysis of the connector with a mechanical coupler, focusing on the local behaviour of the tapered threaded connection between the mechanical coupler and rebar anchor.

1 Introduction

The combination of structural steel and reinforced concrete elements in composite and mixed civil engineering structures arose from the desire to reduce costs and shorten construction timelines. The behaviour of such structures significantly depends on the behaviour of the connection between the steel and RC components which is realised by the use of mechanical connecting devices, i.e., connectors. These connectors are most commonly loaded with shear, tension, or combined loads.

Traditionally, headed studs continuously and uniformly welded along the flanges of steel profiles have provided the connections between structural elements made of steel and reinforced concrete (see Figure 1(a)). The reason lies in the quick execution using automatic welding and their adequate and reliable behaviour under shear, tension, and their interaction, which has been proven by numerous experimental and numerical studies [2,3]. In contrast to welded studs, demountable connectors enable relatively simple disassembly and reuse of structural elements and even entire structures after the "first service life". Over the past few decades, several experimental and numerical studies on the performance of various types of demountable connectors have been performed, the most common of which are shown in Figures 1(b)-1(d). In terms of shear behaviour, it was concluded that these connectors have a comparable load-bearing capacity to welded-headed studs but significantly lower stiffness as well as ductility. It was observed that the stiffness of the connector increased with

the addition of one or two embedded nuts. In terms of tensile behaviour, it was concluded that the failure modes and load capacities of demountable-headed connectors are similar to those of welded studs [1].

Over the last few years, different research groups have analysed the application of demountable shear connectors with bolts and mechanical couplers, which are most commonly used for rebar splicing in RC structures. These connector types are shown in Figures 1(e) and 1(f). The connection between the steel and RC element is achieved on the construction site by screwing the short bolt into the coupler, which was previously embedded in the RC element. The connector can be anchored to the RC element by connecting the coupler with another longer bolt [4,5] or by connecting it with the rebar anchor [6,7]. According to research results, the shear behaviour of these connectors was similar to that of bolts with embedded nuts. It was pointed out that under the action of longitudinal shear, regardless of the connector anchoring method, deformation predominantly occurs in the short bolt. At the same time, mechanical couplers provide a flat surface for the RC element at the place of the connector, making disassembly easier compared to other demountable connector solutions.

In the case of tensile force, connectors with mechanical couplers have a more complex behaviour compared to other connectors shown in Figure 1. The reason lies in the fact that connectors with mechanical couplers are, in general, formed by joining three elements of different mechanical and geometric characteristics (see Figures 1(e) and 1(f)). Therefore, their behaviour in tension, and thus under

^{*} Corresponding author:E-mail address: ivanm@imk.grf.bg.ac.rs

combined load, depends on the behaviour of the “weakest link” in the connector. For example, during the tensile tests conducted on the connectors used by Yang et al. [4] significant deformation occurred in the mechanical couplers. On the other hand, in connectors with mechanical couplers and rebar anchors, the rebar anchor can be the weakest link if high-strength bolts are used [7].

This research aims to analyse the local tensile behaviour of the connector formed by connecting the bolt, mechanical coupler, and rebar anchor (Figure 1(f)). For this purpose, the tensile test was conducted on the connector itself using the tensile testing machine, continuously measuring the load and deformation of the connector at characteristic zones. Based on the load test results, a nonlinear finite element analysis (FEA) analysis of the connector with a mechanical coupler was carried out by the Abaqus software, with an emphasis on modelling the connection between the mechanical coupler and the rebar anchor.

2 Experimental analysis

2.1 Experimental program and material properties

To study the tensile behaviour and determine the corresponding load-bearing capacity of the threaded splice connection between bolt and rebar anchor, tests were performed on a 300 kN capacity Shimadzu tensile testing machine. The connectors were formed by M20 bolts and Ø16 rebar connected to the coupler by ISO coarse metric thread and conical thread, respectively (see Figure 1(f)). The tested mechanical properties of demountable connector components are presented in Table 1.

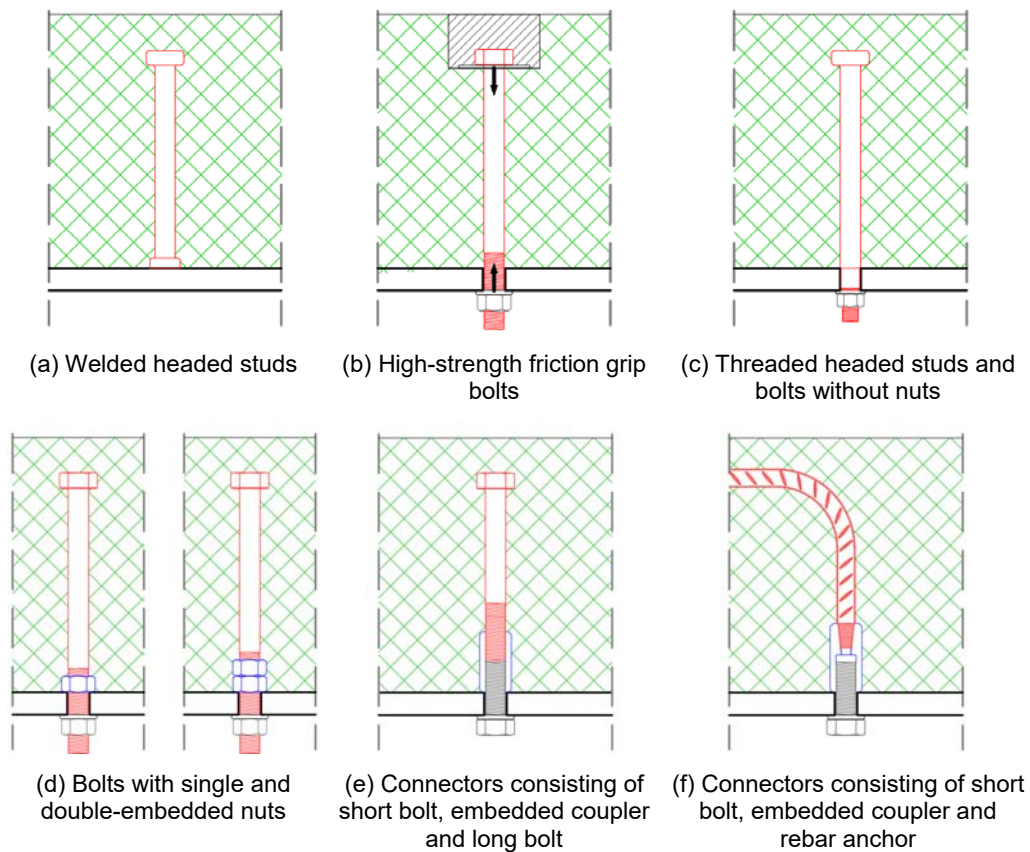


Figure 1. Examples of different types of connectors

Table 1. Tested mechanical properties of demountable connector components

Component	Elastic modulus E (GPa)	Offset yield strength $f_{0.2}$ (MPa)	Tensile strength f_u (MPa)	Ultimate strain ϵ_u (%)
Bolt M20	204.3	855.2	930.6	16.19
Mech. coupler	206.6	770.1	846.0	6.94
Rebar Ø16	193.3	554.7	668.4	19.65

2.2 Test set-up and measurement procedure

The tensile test layout with measuring point arrangement is presented in Figure 2. In total, two samples were tested. The bolts were preloaded to around 20% of the full preload force, according to [8]. The specimens were loaded in displacement control mode with a 1.0 mm/min stroke rate. Global and local deformation were measured in two ways: (1) measurement at discrete points using inductive displacement transducers, strain gauges, and extensometer, and (2) measurement by Digital Image Correlation, DIC.

In the first case, the rebar elongation was measured by an extensometer with a gauge length $l_{ext} = 100$ mm. The displacement of specimens along the loading axis (labelled as d), was measured by inductive displacement transducers at 6 points, relative to the fixed position. Rebar-coupler slip values $\delta_{1,1}$ and $\delta_{1,2}$ were estimated as the subtraction of measured values $d_{1,1}$ and $d_{1,2}$ and $d_{1,3}$ and $d_{1,4}$, respectively. The mean of rebar slip values $\delta_{1,1}$ and $\delta_{1,2}$ was labelled as δ_1 . Similarly, separation between the coupler and bolt grip δ_2 was estimated. This separation was used for estimation of bolt strain ϵ_b along the 24 mm grip length. Coupler strain ϵ_{co} was measured by strain gauges at the weakest section – between bolt and rebar, as shown in Figure 1(f).

In the DIC method, digital images of the front side of the connector were captured at different deformation states and post-processed by matching the same points (or pixels) between the two images recorded before and after deformation. The front side of the connector was painted with white paint. Random speckle pattern was achieved with black paint by hand spraying using the small pipe on the spraying can lid. The acquisition of the digital images during the experiment was performed with a full frame Canon 6D (sensor 36x24 mm, resolution 20.2 megapixels) with a

Canon EF 24-105 mm f/4L IS II USM telephoto lens. The focal length was fixed at 105 mm with f/8 aperture. The camera was placed on a tripod at 0.96 m from specimen in an average spatial resolution of 0.06 mm/pixel. The camera was triggered automatically at time increments of 10 s. DIC analysis was done using an open-source 2D MATLAB program – Ncorr [9].

2.3 Results of tensile tests

The appearance of the connector before, during and after the tensile test is shown in Figure 3. Both specimens failed due to the stripping of taper threads on the end of the rebar. As the coupler and bolt deformation were negligible, they could be easily demounted after testing (Figure 3(c)).

Experimental test results are graphically presented in Figure 4. The maximum force of samples 1 and 2 subjected to the tension was $T_{u,1} = 128.7$ kN and $T_{u,2} = 129.9$ kN, which is about 4% less than the load capacity of the control rebar. In Figure 4(a) stroke Δ_{st} and rebar elongation within free length Δ_{at} are presented as a function of tensile force T . Rebar elongation Δ_{at} was obtained by scaling the elongations measured by an extensometer. On graphs, four characteristic points can be identified as: „Y“ – yield point, „S“ – beginning of rebar strain hardening, „U“ – the ultimate load of the rebar and connector as a whole and „R“ – connector failure. By observing the graphs, it can be concluded that the displacements Δ_{st} and Δ_{at} differ significantly in the rebar’s elastic region due to the wedging of wedge grips into the bar and the bolt fixture. The elastic elongation of the bolt and the mechanical coupler contribute far less to that difference, as confirmed by the small, reversible strains of these two elements (Figure 4(b)).

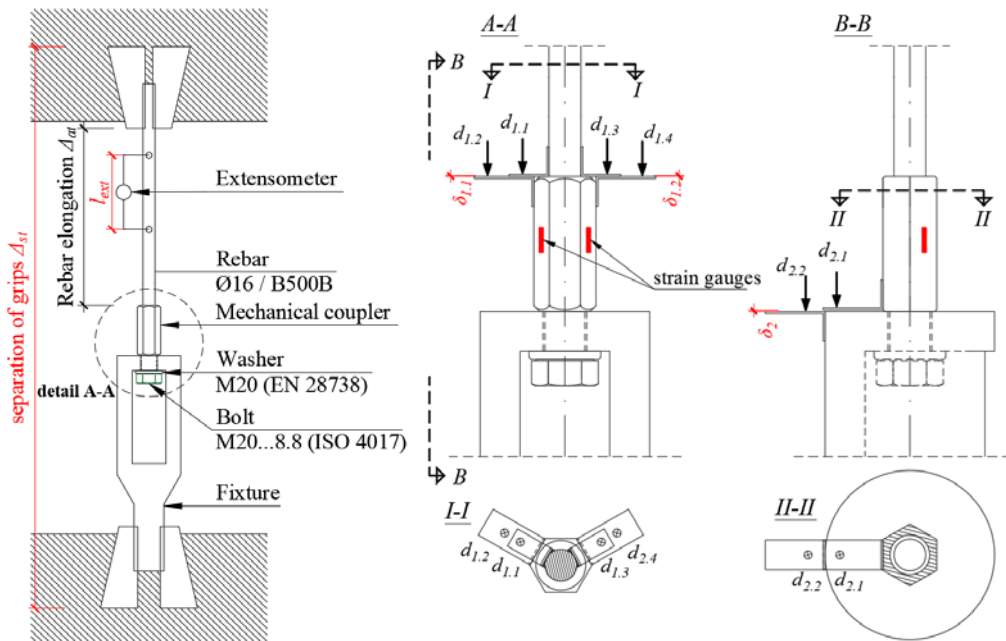


Figure 2. Tensile test layout of threaded splice connection between bolt and rebar – the physical quantities of interest are displayed in red

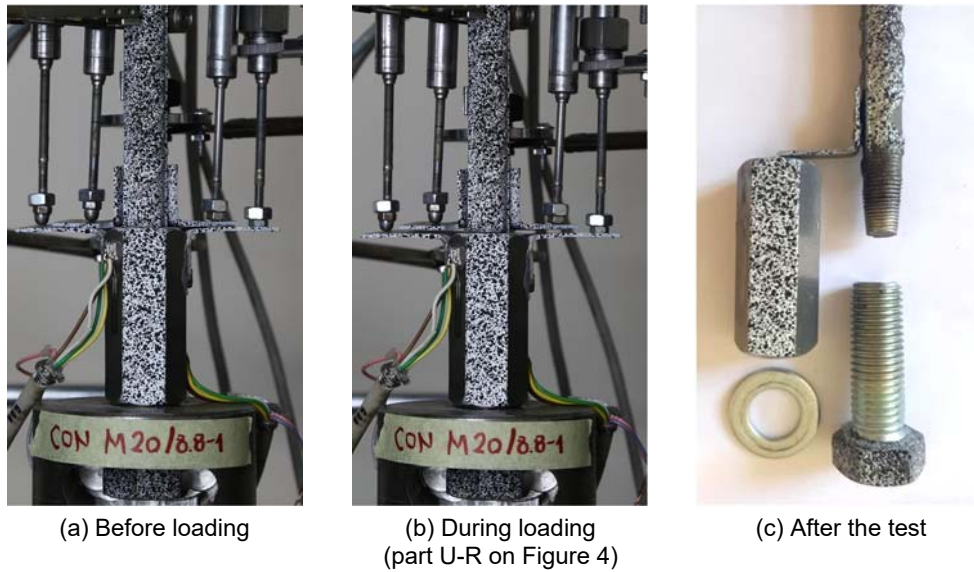


Figure 3. Connector appearance before, during and after the tensile test

After that, the difference between Δ_{st} and Δ_{at} is practically negligible until the connector's load-bearing capacity is reached. Test results showed that the behaviour of the connector as a whole corresponds to that of the control rebar (Figure 4(d)). Reaching the ultimate load of the connector coincides with the onset of stripping of the taper thread on

the rebar inside the mechanical coupler. The result was the rebar anchor slipping out from the mechanical coupler and the increased measured values δ_r on the U-R part, as shown in Figure 4(c). In this area, there is no additional increase of rebar anchor strain, which is illustrated by the line U-R' in Figures 4(a) and 4(d).

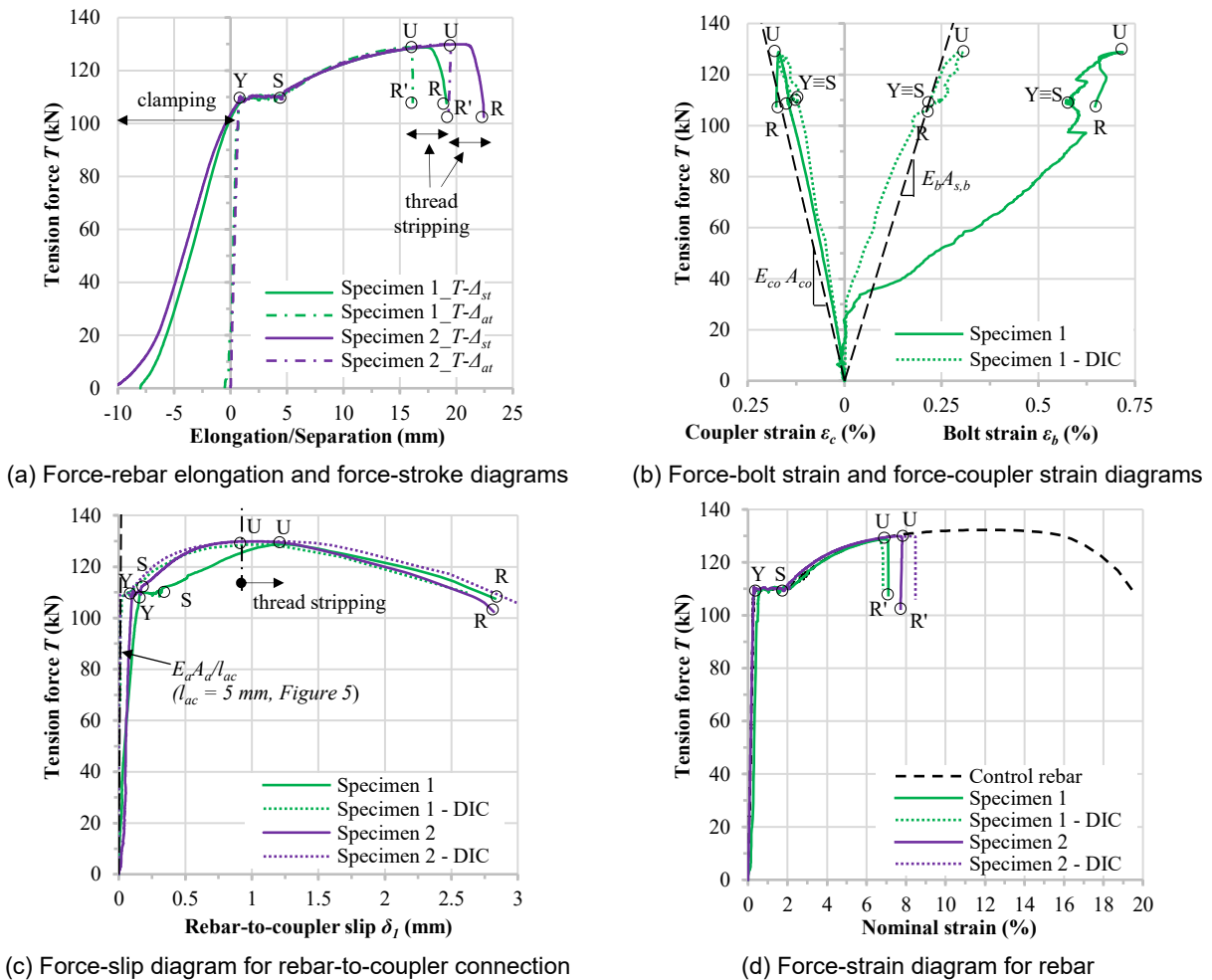


Figure 4. Tensile test results of the connector with a mechanical coupler

Measurement results of $\bar{\delta}_1$ and $\bar{\delta}_2$ in the elastic region deviated to a certain extent from the theoretically calculated values of the corresponding stiffnesses, as can be seen in Figures 4(b) and 4(c). These deviations are especially emphasised in the case of slip $\bar{\delta}_2$, i.e., bolt strain along the grip length ϵ_b . This can be attributed to the distance of the displacement transducers from the corresponding connections of the connector components, which can be seen in Figure 2(b). As shown in Figures 4(b) and 4(c), the results of DIC measurements matched much better with the theoretical values since the measurements were made at the surface of the connector.

3 Numerical analysis

3.1 Geometry of numerical model and boundary conditions

Numerical analysis of the threaded splice connector was performed in Abaqus finite element analysis (FEA) software [10] using the three-dimensional (3D) model shown in Figure 5. During the model's development, some geometry simplifications were made as opposed to the real geometry of the connector parts. These simplifications are based on the conclusions from the experimental analysis. Due to the elastic behaviour of the bolt during the test, the bolt thread was not explicitly modelled. A constant circular cross-section equal to the nominal stress area in the threaded part was adopted. In addition, the bolt-coupler connection was modelled as rigid, using the „Tie“ constraint. The contact between the bolt, washer, and fixture is modelled as „Hard contact“ in the normal direction and „Penalty friction“ in the tangential direction with a friction coefficient of 0.14, according to [11]. The rebar anchor and mechanical coupler threads were also excluded because of the complex taper

thread geometry on the ribbed rebars (see Fig. 3(c)). The connection between the rebar and mechanical coupler was modelled by an idealised conical contact surface, as shown in Figure 5. The contact length of 25 mm was assigned, which is less than the total length of the rebar inside the coupler. The reason for this was the absence of a complete thread on the upper part of the rebar anchor. The rebar-coupler connection was modelled in two ways: as a rigid connection („Tie“ constraint) and by „Cohesive contact“ formulation, according to [10].

3.1.1 Modelling of rebar-to-coupler contact

For modelling rebar-to-coupler contact, the cohesive contact formulation was used. According to [10], cohesive contact between two surfaces was defined by the relation between the nominal traction stress t as a function of the separation (slip) of the surfaces δ , as shown in Figure 5. The behaviour of this connection includes four characteristic parts: $0-i$ – elastic part, i – damage initiation, $i-f$ – damage development and f – connection failure. The uncoupled stress-separation relationship defines the elastic behaviour of the contact:

$$t = \begin{Bmatrix} t_n \\ t_s \\ t_t \end{Bmatrix} = \begin{bmatrix} K_n & 0 & 0 \\ 0 & K_s & 0 \\ 0 & 0 & K_t \end{bmatrix} \begin{Bmatrix} \delta_n \\ \delta_s \\ \delta_t \end{Bmatrix} \quad (1)$$

whereby:

- t_n, t_s, t_t normal, tangential and longitudinal nominal traction stress,
- $\delta_n, \delta_s, \delta_t$ normal, tangential and longitudinal separation,
- K_n, K_s, K_t normal, tangential and longitudinal stiffness.

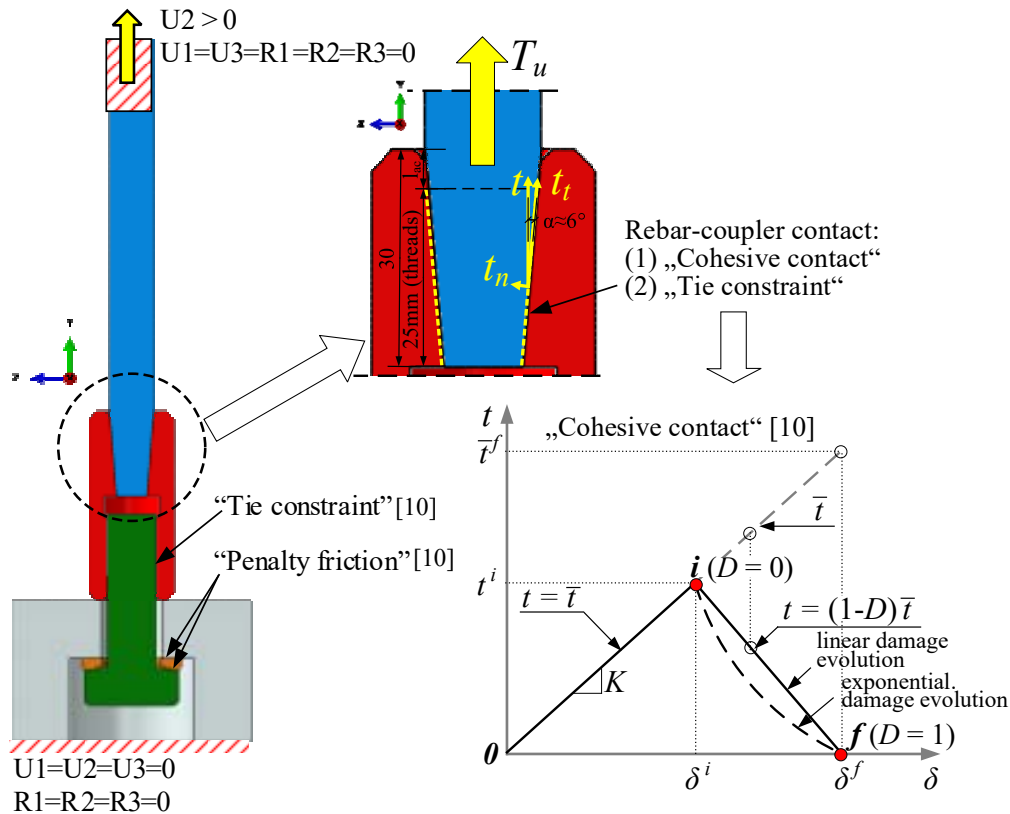


Figure 5. Numerical model geometry and boundary conditions of the connector with a mechanical coupler

Degradation and failure of the contact between two surfaces are defined by the damage initiation criterion, the damage evolution function (law), and the maximum separation. Damage initiation criteria can be defined by the corresponding maximum stress (t^i) or maximum separation (δ^i) from Equation (1). In general, the damage development function can have an arbitrary form. As an example, linear and exponential damage evolution functions are shown in Figure 5. Regardless of shape, the damage evolution function depends on the scalar quantity named damage parameter D , which represents the main input parameter during the definition of degradation and failure of contact in Abaqus software [10]. The damage parameter has a value of $D = 0$ at the maximum stress and a value of $D = 1$ at the maximum separation of the connection. As can be concluded from equation (1), all three components have different behaviours in the elastic region. However, after fulfilling the damage initiation criteria for any of the components (directions) of the connection, damage occurs in all three directions in line with the same damage evolution law.

In this study, the properties of the cohesive contact between the rebar and coupler were defined based on the experimentally determined force-slip relation ($T-\delta_t$), as shown in Figure 4(c). Considering the small inclination of the conical thread generatrix (see Figure 5), the main parameters for defining the behaviour of the contact are the longitudinal stress t_t and the longitudinal separation δ_t . The value of $K_s = K_n = K_t = 10000$ MPa/mm was determined iteratively and adopted for connection elastic stiffness to match the test result obtained by DIC method. The initiation criteria was defined by maximum longitudinal stress $t_t^i = 128$ MPa. The value of this stress is approximately equal to the value obtained by dividing the connector load capacity T_u by the contact area and by the projection on the generatrix, as shown in Figure 5. The linear damage evolution with the maximum longitudinal traction $\delta_t^f = 2.0$ mm was considered and adopted based on the test results (part U-R). For the other two directions, the same connection properties were used. Figure 6 shows the adopted cohesive contact characteristics.

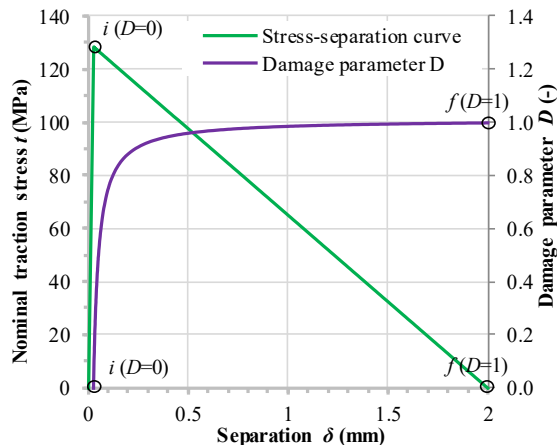


Figure 6. Cohesive contact for modelling rebar-to-coupler connection

3.2 Material models

The Poisson's ratio of 0.3 and a density of 7850 kg/m³ were set for all steel materials. The material model of the bolt, coupler, and rebar anchor was adopted following the properties shown in Table 1. For the bolt, mechanical coupler, fixture, and washer the modulus of elasticity $E_0 =$

210 GPa was adopted. Taking into consideration negligible permanent deformation of couplers and bolts during loading, a bilinear elastoplastic stress-strain relation was adopted, while completely elastic behaviour was adopted for the fixture and washer. For reinforcement, the modulus of elasticity $E_0 = 200$ GPa was adopted. The behaviour of the rebar anchor was modelled based on the stress-strain curve of the control rebar without taking into account the descending branch. Figure 7 shows the adopted stress-strain relationships for the bolt, mechanical coupler, and rebar anchor.

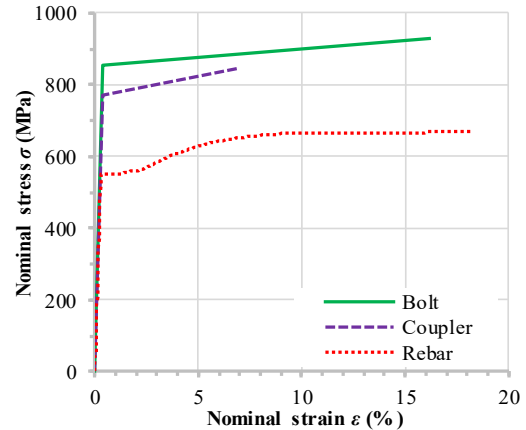


Figure 7. Stress-strain curves for bolt, mechanical coupler and rebar anchor

3.3 Finite element mesh and analysis procedure

Tetrahedral finite elements (C3D4) were adopted for all connector components. The bolt, washer, mechanical coupler, and rebar anchor were modelled with 1.5 mm finite elements, while the bolt grip was modelled with 3 mm finite elements. A sensitivity analysis of FEA model's global behaviour was performed by using the 1 mm, 1.5 mm, 2 mm and 3 mm finite elements representing the connector.

For nonlinear quasi-static analysis, the Abaqus/Explicit solver was used [10]. The displacement U2 was applied at the top of the specimen (Figure 5) at a time interval of 100 s. The mass scaling method with a desired time increment of 0.002s was used to increase calculation speed.

3.4 Result of FE analysis

Nonlinear FEA results of the threaded splice connector subjected to tension are shown in Figure 8. Considering the failure mode identified during the connector tensile test, a comparison was made between the rebar force-slip and force-strain curves. Modelling the rebar-coupler contact with a rigid connection („Tie“ constraint) describes relatively well the connector behaviour until the yield point (Y) of the rebar anchor, as shown in Figures 8(a) and 8(b). After the rebar yield point, there are clear differences between the experimental and FEA results. In the latter, the connector failure was caused by rebar tensile failure (see Figure 8(b), part U→R). As can be seen from the figures, a good match between the test results and FEA results of the model with cohesive contact was achieved in the rebar-to-coupler slip branch up to 0.7 mm (up to the maximum load). At larger values of slip δ_t , contact damage occurs in accordance with the adopted linear damage evolution (part U-R), which is characterised by a faster drop in tensile force compared to

the experimentally obtained results. Although a better model behaviour on the descending branch of the force-slip curve can be obtained by defining a more accurate damage evolution law (trilinear, parabolic, etc.), the presented model well describes the global behaviour of the connection. In the case of the FEA model with cohesive contact, rebar pull-out failure mode occurred due to contact failure. Also, as can be seen from the graphs, the behaviour of the connection had low sensitivity to changes in the size of finite elements.

Figures 8(c) and 8(d) show a comparison of von Mises stress distribution in the connection of a mechanical coupler and a rebar anchor at various levels of tension load, based on FEA models with „Tie“ constraint and a „Cohesive contact“ model, respectively. The tensile force levels corresponding to the yielding point of the rebar anchor and the load capacity of the connector were analysed. It can be concluded that with a rigid connection, the tensile force is dominantly transmitted in the upper part of the mechanical coupler, regardless of the load level. On the other hand, by modelling the connection with cohesive contact, rebar-coupler force transmission is more uniform up to the rebar yield point. After that, the thread damage occurs in the higher part of the rebar, and the force transmission zone moves towards the lower part, i.e., the free end of the rebar. This fact is supported by the distribution of von Mises stress at the maximum tensile force, presented in Figure 8(d). Similar to

the experimental analysis, the failure of the connector was caused by the loss of contact between the coupler and the lower part (end) of the rebar.

4 Conclusions

In this paper, the tensile behaviour of a demountable connector consisting of a bolt, mechanical coupler, and rebar anchor was analysed. Tensile test results showed that the behaviour of the rebar, as the weakest component, has a significant influence on the behaviour of such a connector as a whole. The tensile load capacity of the tested samples was approximately equal to that of the control rebar ($T_u = 129.3$ kN). Both samples failed due to rebar pull-out from the mechanical coupler, as a result of the conical thread stripping on the rebar anchor.

The connector's nonlinear three-dimensional finite element model was created and calibrated using the results of experimental tests. Particular focus was placed on modelling the connection between the mechanical coupler and rebar anchor. It was shown that the complex behaviour of this connection, up to the connector load capacity, can be adequately represented by applying the cohesive contact model in Abaqus software [10], whose application and parameters are described in detail.

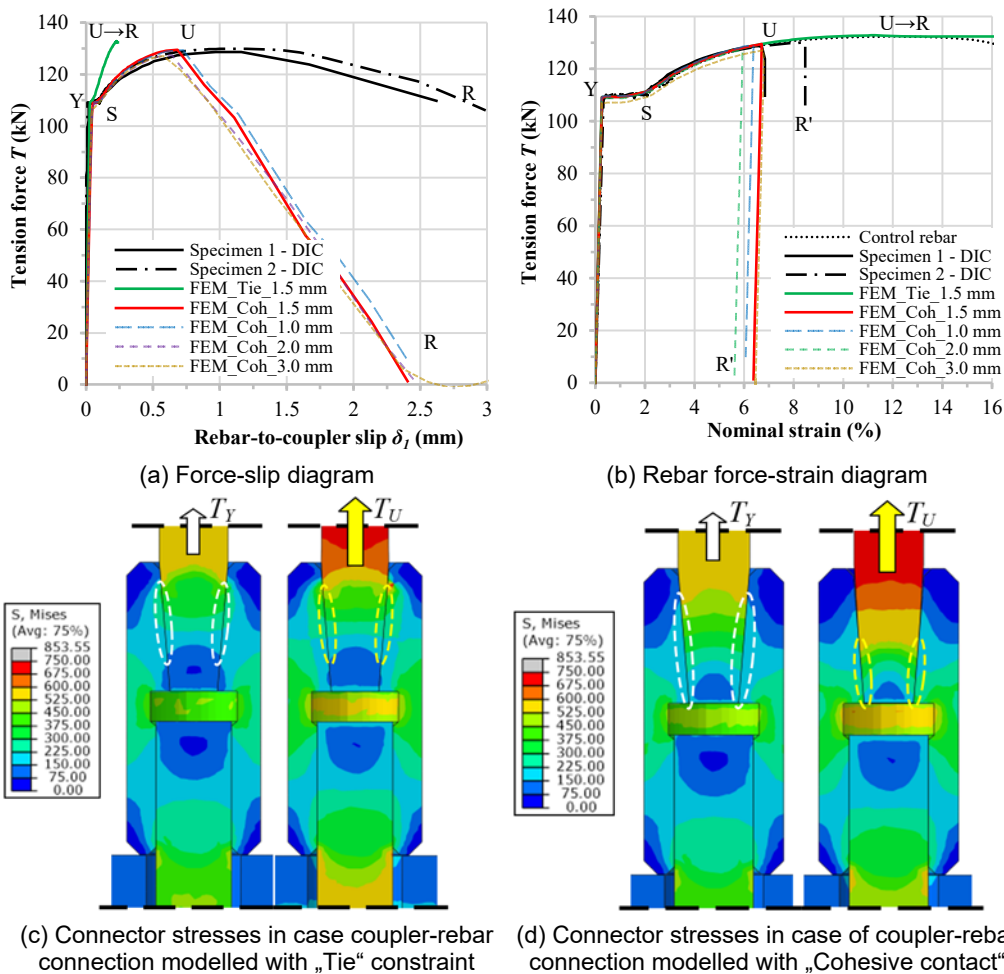


Figure 8. Tensile FEA results of the connector with mechanical coupler

Acknowledgement

The authors would like to express their gratitude to the Ministry of Education, Science, and Technological Development of the Republic of Serbia for the financial support within Project 200092.

References

- [1] EN1992-4, Eurocode 2: Design of concrete structures - Design of fastenings for use in concrete. Brussels: CEN, 2018.
- [2] L. Pallarés and J. F. Hajjar, "Headed steel stud anchors in composite structures, Part II: Tension and interaction," *J. Constr. Steel Res.*, vol. 66, no. 2, pp. 213–228, 2010, doi: 10.1016/j.jcsr.2009.08.008
- [3] L. Pallarés and J. F. Hajjar, "Headed steel stud anchors in composite structures, Part I: Shear," *J. Constr. Steel Res.*, vol. 66, no. 2, pp. 198–212, 2010, doi: 10.1016/j.jcsr.2009.08.009
- [4] F. Yang, Y. Liu, Z. Jiang, and H. Xin, "Shear performance of a novel demountable steel-concrete bolted connector under static push-out tests," *Eng. Struct.*, vol. 160, no. December 2017, pp. 133–146, 2018, doi: 10.1016/j.engstruct.2018.01.005
- [5] Kozma, C. Odenbreit, M. V. Braun, M. Veljkovic, and M. P. Nijgh, "Push-out tests on demountable shear connectors of steel-concrete composite structures," *Structures*, vol. 21, no. Asccs, pp. 45–54, 2019, doi: 10.1016/j.istruc.2019.05.011
- [6] B. Milosavljević, I. Milićević, M. Pavlović, and M. Spremić, "Static behaviour of bolted shear connectors with mechanical coupler embedded in concrete," *Steel Compos. Struct.*, vol. 29, no. 2, pp. 257–272, 2018, doi: 10.12989/scs.2018.29.2.257.
- [7] I. Milićević, B. Milosavljević, M. Pavlović, and M. Spremić, "Bolted connectors with mechanical coupler embedded in concrete: Shear resistance under static load," *Steel Compos. Struct.*, vol. 36, no. 3, pp. 321–337, 2020, doi: 10.12989/scs.2020.36.3.321.
- [8] EN1993-1-8: Eurocode 3: Design of steel structures. Part 1-8: Design of joints. Brussels, Belgium: European Committee for Standardization (CEN); 2005
- [9] Blaber, J., Adair, B., Antoniou, A., 2015. Ncorr: Open-Source 2D Digital ImageCorrelationMatlab Software. *Exp. Mech.* 55, 1105–1122.
- [10] ABAQUS User Manual. Version 6.12. Providence, RI, USA: DS SIMULIA Corp; 2012.
- [11] ECCS Publication No38 - European Recommendations for Bolted Connections in structural steelwork. Brussels, Belgium: ECCS; 1985